

HOT DUCTILITY AND FRACTURE OF HYPEREUTECTIC AlSiNi PM ALLOY

S.T. Mandziej, J. Ďurišin

Abstract

Hypereutectic AlSiNi-alloys having low density, high strength-to-weight ratio and good wear resistance are prospective candidates for new automotive, aerospace and household applications. As they are manufactured in a PM process from rapidly solidified multi-phase powders, and their advantageous application properties very much depend on this initial process, the net-to-shape forming of these alloys has certain limitations. In particular, these alloys are brittle at ambient temperatures, while during too long exposure at temperatures close to solidus they loose their advantageous properties. To evaluate their best forgeability "window", the hot/warm mechanical properties of these alloys were studied by means of physical simulation. In particular, their flow-stress properties, dimensional stability and critical strains to fracture were determined, as well as the fracture modes were identified.

Keywords: PM Al alloys, mechanical properties, microstructure

INTRODUCTION

Aluminium-silicon alloys are known of many applications in as-cast and machined form for machine components requiring good strength-to-weight ratio and wear resistance when exposed to elevated temperatures like e.g. pistons in automotive engines. Advantageous mechanical properties of these alloys, in particular stiffness and wear resistance increasing with silicon content, led to development of hypereutectic alloys with amount of Si exceeding 20%. Introduction of other alloying elements to the system, in particular of nickel, resulted in such an exceptional composition like the Al-27Si-6Ni PM alloy [1], which is the subject of this study. The usual manufacturing method of such alloy is a rapid solidification from melt followed by hot sintering / extrusion of the rapidly solidified powder to form sound billets or pre-forms of high density.

For successful industrial applications of this type alloys high efficiency manufacturing requires their forming into components by an accurate net-shape or near-net-shape process, like e.g. precision forging, with minimum if any post-forming operations.

In the previous EU project "MicroAlu" in the INCO-Copernicus programme of 1997-99, the hot/warm formability of these alloys was studied by means of physical simulation [2]. Thermal-mechanical simulator Gleeble 3500 [3] was used to measure physical and mechanical properties of the investigated material at the conditions simulating these of the real industrial manufacturing processes. In particular, the flow-stress properties, dimensional stability as well as critical strains to fracture were determined at different heating cycles and deformation rates.

The actually presented information about the microstructure and fracture modes of this alloy has been a part of an extension study after the "MicroAlu" project. In the result of

this study and due to fruitful interactions with international partners, a successful application in the 5th FP GROWTH programme of the EU was made and a project was launched aiming for industrial applications of household and automotive components made of the hypereutectic AlSiNi and similar PM alloys.

MECHANICAL CHARACTERIZATION

The Al-27Si-6Ni PM alloy of this study was made of rapidly solidified powder hot/warm extruded into 16 mm diameter rods and from these rods samples were taken for investigations. In such as-delivered form the alloy had very low ductility at room temperature: its true (logarithmic) strain to fracture in uniaxial compression of cylindrical specimen did not exceed 0.08 even for the strain rate as low as 0.0001 sec^{-1} . As from the previous research it was also known that during processing at temperatures above 480°C the alloy loses its advantageous application properties [4], it appeared necessary to seek for an optimum formability range at elevated temperatures lower than 480°C . This temperature determines the practical upper limit of the formability range, while the beginning of the formability range coincides with the stress relaxation temperature i.e. with the “softening” of the alloy during its heating up after cold deformation. To determine this last, a simple force relaxation test was used on Gleeble.

Force relaxation tests

The test carried out on cylindrical samples comprised an axial “cold” compression followed by temperature cycle of heating up to 485°C with a rate of 10°C/sec and recording of force exerted on the sample during the thermal cycle with fixed position of Gleeble’s anvils. Each applied compression was of 0.005 total strain with the strain rate 1 sec^{-1} . Single-cycle and multi-cycle tests were carried out. In the multi-cycle procedure, after cooling the sample down to about 100°C , the next compression and then heating cycle were applied.

The initial strain of each cycle was exerting an initial force on the sample and during heating-up of the sample between fixed anvils this force at first was increasing due to expansion of the sample while later it stabilized and finally dropped down due to softening and recrystallization of the sample’s microstructure. The beginning of the formability, i.e. of the potential warm forging range, is around the “top” of relaxation curve recorded in this way, while the optimum hot working range should be above the temperature at which the force relaxes to its minimum.

This force relaxation procedure, of applying the multiple thermal-mechanical cycles with different peak temperatures, was also used to study the thermal stability of the alloy. An example given in Fig.1, shows four subsequent force relaxation curves of the Al-27Si-6Ni PM alloy. It can be seen that after each thermal cycle the material strengthens a bit and the peak of the maximum force moves to higher temperatures. As this could have been an effect of the thermal-mechanical cycles on the microstructure and mechanical properties of the alloy, the more accurate study of the thermal stability was carried out by means of a crosswise contact-less laser dilatometer on Gleeble. The following Fig.2 shows permanent expansion of a 16 mm diameter sample after 10 thermal cycles with peak temperature of 475°C . The heating rate was 2°C/sec with no soaking at peak temperature. When the peak temperature of such thermal cycling was 425°C or lower, the permanent expansion was negligible, while for the peak temperature of 450°C the alloy, after a small initial expansion in the first 3 to 5 thermal cycles, in the subsequent cycles stabilized and did not expand further.

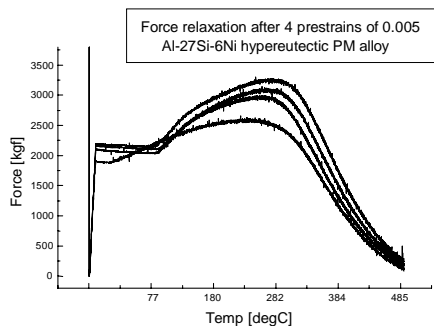


Fig.1. Force relaxation of Al-27Si-6Ni during 4 thermal cycles after pre-strains of 0.005.

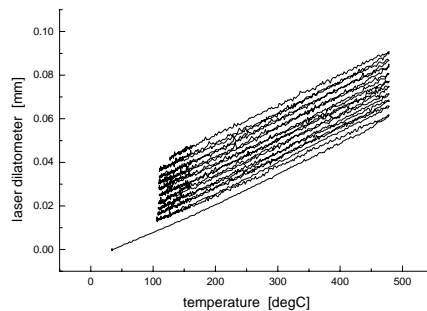


Fig.2. Dimensional instability of Al-27Si-6Ni alloy during 10 thermal cycles to 475°C .

Strain to fracture

To measure the critical strain to fracture, uniaxial compression tests were carried out on cylindrical specimens of 12 mm diameter. The specimens were compressed between tungsten carbide anvils, at temperatures from 350°C to 500°C, after heating from room temperature with the rate of 20°C/sec and soaking for 10 sec. The compression was exerted with a constant strain rate of 1/sec in a single stroke, till occurrence of radial cracks at the largest perimeter of the sample, Fig.3. After the cracks appeared, their total widths were measured and the critical strain to fracture was calculated as: $\epsilon_{cr} = 2 (\ln D_{cr} - \ln d)$, in which d is the initial diameter of the sample and $D_{cr} = D - \Sigma c_i / \pi$ is the critical diameter of the cracks appearance while Σc_i is the sum of the opened crack widths along the maximum perimeter of the compressed and thus bulged sample, and D is the maximum diameter after the compression.

The results of these measurements are given in Fig.4, showing a maximum around 425°C.



Fig.3. Cylindrical samples used to determine strain-to-fracture.

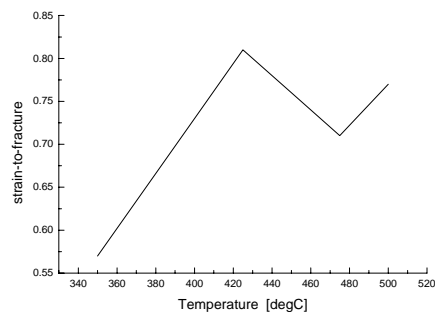


Fig.4. Strains-to-fracture of Al-27Si-6Ni alloy at temperatures from 350 to 500°C.

Plane strain compression tests

To measure flow stresses of the Al-27Si-6Ni PM alloy, plane strain compression tests were carried out at various strain rate / temperature conditions. The test temperatures were from 350 to 500°C and applied strain rates from 0.001 sec⁻¹ to 100 sec⁻¹. Some examples of stress-strain curves are given in Figs.5-7, and a summary of results is given in Tab.1. The plane strain samples were deformed to the true strain of 1.2 or higher, no wonder that for the lower of the applied deformation temperatures at higher strain rates numerous of the samples developed cracks. For medium and high strain rates, i.e. 1/sec and higher, see Figs.5 and 6, the flow stress curves are of a typical dynamic recovery and recrystallization character, which means that after the initial high strain hardening (to strains between 0.1 and 0.2) later the flow stress decreases and stabilizes. The drop of the flow stress is higher for lower deformation temperatures and smaller for higher temperatures; it is substantial for higher strain rates, as it is certainly affected by the heat generated during the compression test, Fig.7. At very low strain rates and long deformation times the precipitation processes as well as transformations of unstable phases of this alloy result in characteristic serrations on the flow stress curves. Simultaneously, the alloy becomes well deformable at relatively low flow stresses, Fig.8, but its final room temperature application properties become poorer [2].

MICROSTRUCTURAL CHARACTERIZATION

The hot cracks formed at the perimeter of the strain-to-fracture samples as well as the hot cracks appearing at the end portions of the deformation zone on plane strain specimens were examined by light microscopy and by scanning electron microscopy. The character of the dynamic flow stress curves and the substantial deformation heat generated in the specimens suggested that adiabatic shear bands play a substantial role in the deformation and fracture of this alloy. In the previous research work it was observed that the microstructure, as seen by light microscopy, did not differ too much between the as-delivered state and the hot/warm deformed states [2], however the final properties after the forming were much different than before the deformation. Thus, the search for these shear-bands and finding of their role in the hot/warm deformation and fracture has become one of the aims of this work.

Tab.1. Summary results of flow stress and dynamic E modulus.

plane strain rate [1/sec]	testing temperature [°C]	dynamic E – modulus [10 ³ MPa]	maximum flow stress σ_{ym} [MPa]	flow stress for $\varepsilon = 0.3$ $\sigma_{v0.3}$ [MPa]	flow stress for $\varepsilon = 0.6$ $\sigma_{v0.6}$ [MPa]	flow stress for $\varepsilon = 1.0$ $\sigma_{v1.0}$ [MPa]
0.001	350	3.29	137	121	125	136
	380	2.06	87	82	85	81
	420	1.87	75	64	70	74
	460	1.02	59	40	48	54
0.1	350	2.14	208	191	200	201
	380	1.66	172	160	162	161
	420	1.36	126	122	123	119
	460	0.81	80	71	75	76
1.0	350	2.12	252	244	206	223
	380	1.97	218	207	193	202
	420	1.97	182	171	166	177
	460	1.76	124	143	122	118
10.0	350	6.37	298	186	218	223
	380	3.09	287	243	240	236
	420	2.65	243	221	198	201
	460	2.13	192	177	175	175

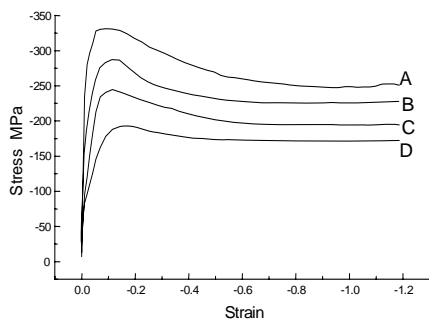


Fig. 5. Flow stress curves for strain rate 10/sec; A - 350°C, B - 380°C, C - 420°C, D - 460°C.

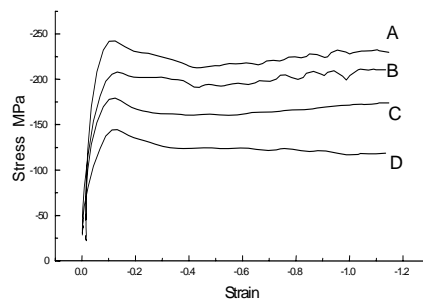


Fig. 6. Flow stress curves for strain rate 1/sec; A - 350°C, B - 380°C, C - 420°C, D - 460°C.

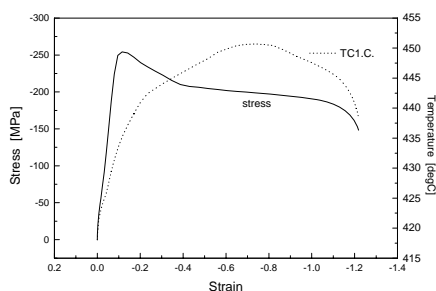


Fig. 7. Flow stress curve for strain rate 30/sec at temperature 420°C and temperature rise on the sample (Tc1).

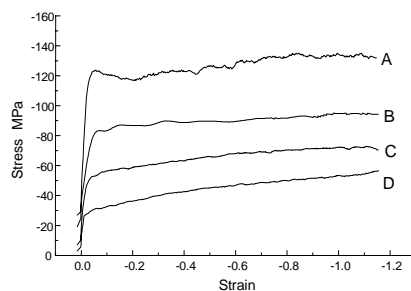


Fig. 8. Flow stress curves for strain rate 0.001/sec; A - 350°C, B - 380°C, C - 420°C, D - 460°C.

Metallography

The initial microstructure of the Al-27Si-6Ni PM alloy, Fig.9, contained equiaxial silicon crystals relatively uniformly distributed in the Al-base matrix and crystals of intermetallic phases like AlNi, Al₃Ni, Ni₃Al as well as silicides NiSi, Ni₂Si, Ni₃Si. Oxides of Al and Si were also present. These phases were identified by X-ray diffractometry elsewhere [2]. Due to the extrusion process of manufacturing the semi-product, some directionality of their distribution could be observed. As the heating of samples to deformation temperatures was relatively fast (10°C/sec) and soaking time was short (30 sec), no changes of this microstructure could be seen by light microscope in non-deformed zones of plane strain samples. However, in the deformed zones slightly pronounced shear bands were observed, especially for lower testing temperatures (350 and 380°C) and strain rates of 10/sec and higher. An example of the shear bands crossing each other from different directions is given in Fig.10.

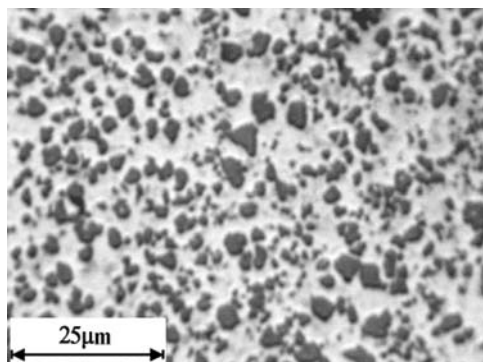


Fig.9. Microstructure in as-delivered state showing silicon and intermetallics in Al-base matrix.

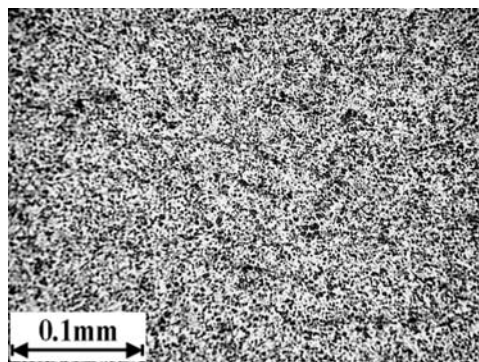


Fig.10. Crisscrossing shear bands in plane strain sample deformed at 380°C with strain rate 30/sec.

On intersections of shear bands at the lowest used deformation temperature (350°C) sometimes micro-cracks were observed, while for higher deformation temperatures certain “refining” of the silicon crystals and other particles appeared, Fig.11. At the lower deformation temperatures and dynamic deformation the developed cracks usually followed the regions of high density of larger-than-average particles, i.e. silicon crystals, Fig.12. With increase of deformation temperature, numerous voids formed ahead of the crack tip and the main crack propagated by coalescence of these voids, Fig.13. At the highest test temperature - at 500°C on the uniaxially compressed sample a large number of micro-cracks formed parallel to the perimeter surface of the sample. They indicated an internal necking ductile damage mechanism and the growth of the main crack appeared by breaking the bridge portions between these micro-cracks, Fig.14.

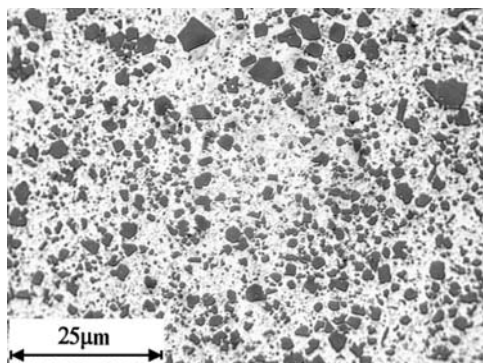


Fig.11. “Refined” Si and intermetallic particles at intersection of shear bands; sample deformed with 30/sec at 380°C.

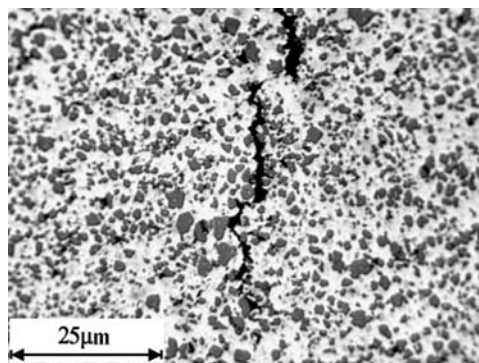


Fig.12. Crack in plane strain sample: 380°C - 30/sec, following a region of larger than average Si particles.

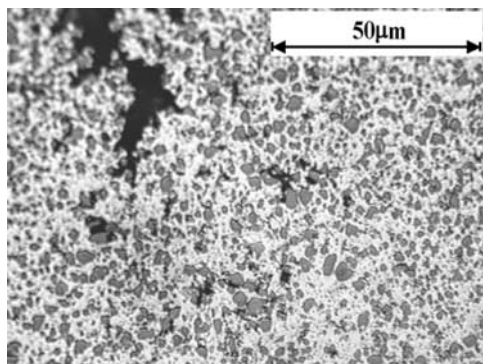


Fig.13. Voids and micro-cracks ahead of the crack tip in a strain-to-fracture sample deformed with the rate 1/sec at 460°C.

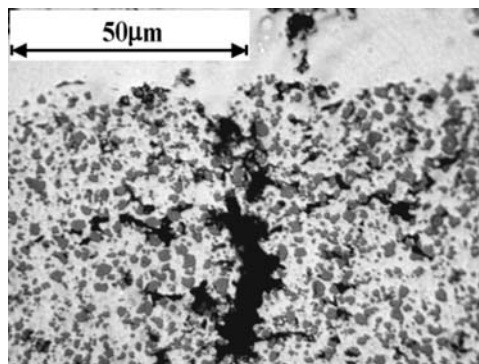


Fig.14. Micro-cracks parallel to the surface in a strain-to-fracture sample deformed with the rate 10/sec at 500°C.

Fractography

Next to the light-microscopic observations of the cracks on cross-sectioned samples, SEM observations of fracture surfaces were carried out.

The shear mode of fracture was dominating in samples deformed at 350°C with strain rate of 1/sec or higher. It also dominated at temperatures 380-420°C for strain rates above 5/sec. On the fracture surfaces shear bands were observed, Fig.15, and on intersections of the shear bands deep secondary cracks appeared, Fig.16. The regions of “refined” second phases formed at the intersections of the shear bands (see Fig.11) appeared to be an obstacle to the crack propagation – the cracks usually by-passed them, Fig.17, and almost no voids could be found in these regions. Most of the voids assisting the crack propagation nucleated at interfaces between Si particles and matrix and the shear-type fracture usually initiated from them, Fig.18.

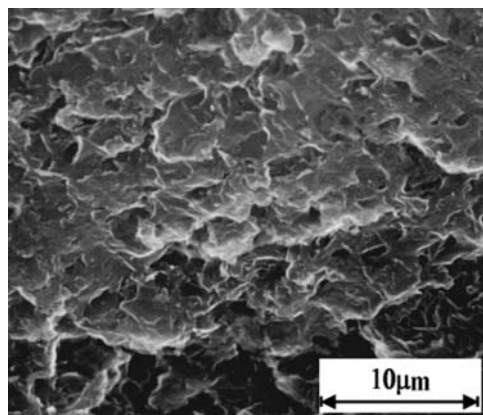


Fig.15. Shear-type fracture showing traces of intersecting shear bands; plane strain compression, 350°C – 1/sec.

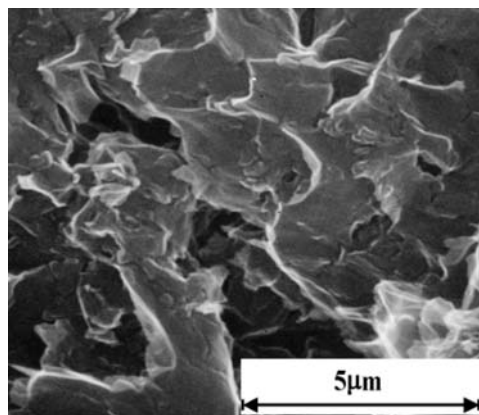


Fig.16. Deep voids and secondary cracks on at intersection of shear bands; plane strain compression, 350°C – 1/sec.

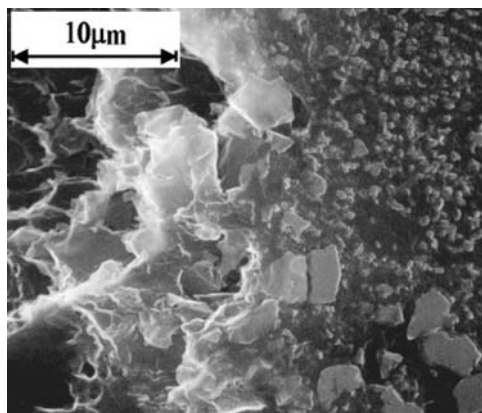


Fig.17. Cross-section through crack by-passing a field of matrix with numerous very fine particles (380°C – 30/sec).

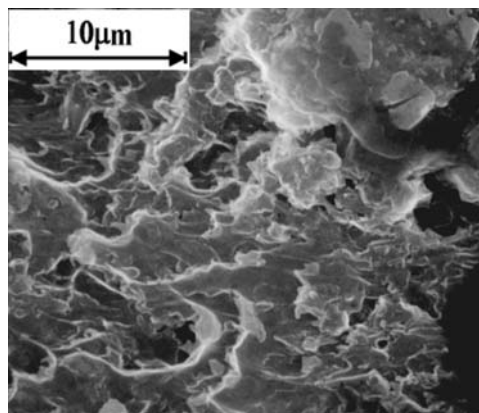


Fig.18. Voids “left behind” larger Si particles on shear fracture surface (380°C – 30/sec).

Fracture of the matrix was generally ductile; the evidences of ductility were everywhere on the shear surfaces and especially within deep secondary cracks in which numerous dimples could be seen, Fig.19. The matrix appeared also very ductile in the bridging portions between the hard second phase particles, Fig.20, forming many dimples with small particles inside.

For the deformation temperatures 460-500°C, even for strain rates higher than 10/sec, the regions with refined second phase particles could not be seen anymore. Instead, shear bands of exceptionally high local ductility were formed, Fig.21. In these bands layers with high density of hard particles were separated from the layers of matrix, while retaining a good cohesion between them, Fig.22. Thus, by the processing with the highest available strain rates at the temperatures of 460-500°C, a “secondary composite” has been formed of peculiar properties.

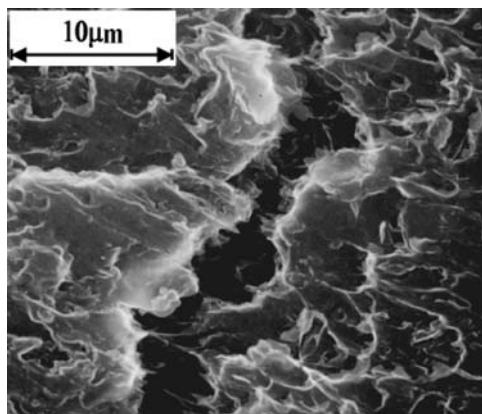


Fig.19. Fibrous-type deep secondary crack intersecting a shear fracture (380°C – 30/sec).

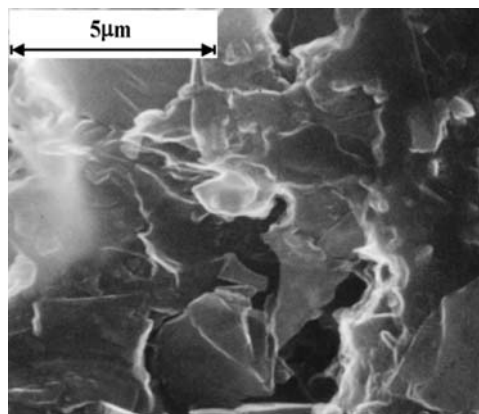


Fig.20. Ductile character of fractured matrix between brittle Si particles (380°C – 30/sec).

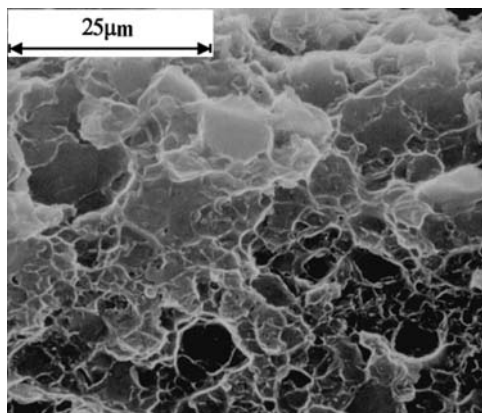


Fig.21. Co-existence of highly ductile dimpled region with brittle cracks of Si particles (460°C - 80/sec).

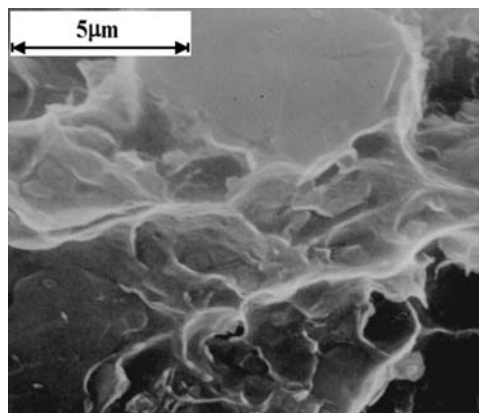


Fig.22. Large Si particle showing high cohesion with surrounding ductile matrix (460°C - 80/sec).

The exceptional properties of this “secondary composite” could be illustrated on the following two pictures: Figs.23 and 24. The very good hot ductility of the matrix layers formed during the processing at temperatures 460-500°C with strain rates of 30/sec and higher, was afterwards retained up to room temperature. Thus, the room temperature fracture of these layers appeared also very ductile. In result of the ductility improvement after the warm forging in this regime, the final mechanical properties of manufactured components were also improved.

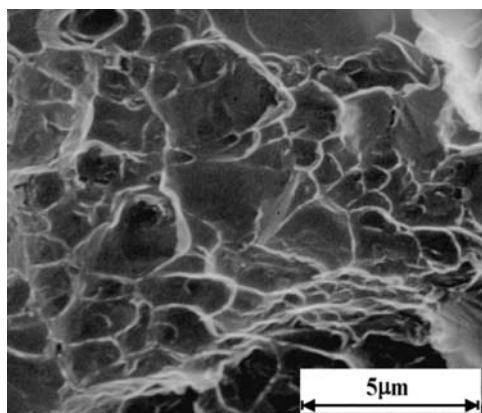


Fig.23. Room temperature fracture of matrix layer after processing at 460°C with 80/sec.

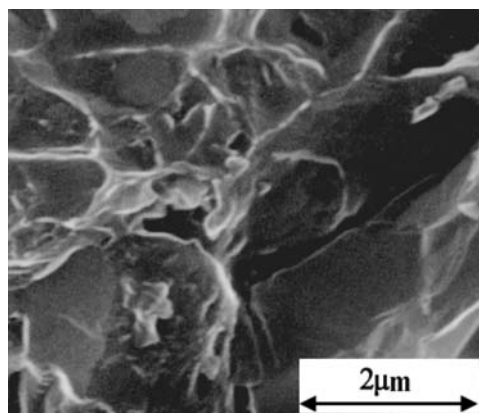


Fig.24. Ductile closing of a void near cracked Si particle RT fracture after processing at 460°C with 80/sec.

CONCLUSIONS

1. During dynamic warm deformation of Al-27Si-6Ni hypereutectic PM alloy hot cracks at temperatures below 400°C are generally due to shear band formation.
2. Dynamic deformation with medium strain rates at temperatures between 380 and 420°C causes locally refinement of second phase particles, thus improving ductility.

3. During high rate processing at temperatures of 460-500°C, the separation of particle-rich layers from layers of matrix while retaining good cohesion between them, results in the formation of “secondary composite” having improved application properties.

REFERENCES

- [1] H.Sano, N.Tokinaze, Y.Ohkubo & K.Sibu; Proc. 2nd Int. Conf. on Spray Forming, Swansea, UK, 1993, paper 4.4.
- [2] “MicroAlu” - Formability Modelling of Aluminium Base PM Alloys, INCO-Copernicus EU Project Nr. CT 96-0750, Final Report, 25.01.1999.
- [3] <http://www.leeble.com>
- [4] G.Ziaja; Technical University of Budapest, 1997, private communication.
- [5] Y.Bai & B.Dodd ; Adiabatic Shear Localization, Pergamon Press, Oxford UK, 1992.

The paper was orally presented during the Int. Conf. DF PM 2002 (Stará Lesná, Slovak Republic, September 15-18, 2002). The conference contribution was extended and revised and have been peer-reviewed.